Sara M. Smith
Department of Mechanical and Aerospace Engineering, Old Dominion University, Norfolk, VA 23529

Justine Marin
Department of Mechanical and Aerospace Engineering, Old Dominion University, Norfolk, VA 23529

Amari Adams
Department of Mechanical and Aerospace Engineering, Old Dominion University, Norfolk, VA 23529

Keith West
Department of Mechanical and Aerospace Engineering, Old Dominion University, Norfolk, VA 23529

Zhili Hao
Department of Mechanical and Aerospace Engineering, Old Dominion University, Norfolk, VA 23529

Radial and Axial Motion of the Initially Tensioned Orthotropic Arterial Wall in Arterial Pulse Wave Propagation

With the arterial wall modeled as an initially tensioned thin-walled orthotropic tube, this study aims to analyze radial and axial motion of the arterial wall and thereby reveal the role of axial motion and two initial tensions of the arterial wall in arterial pulse wave propagation. By incorporating related clinical findings into the pulse wave theory in the literature, a theoretical study is conducted on arterial pulse wave propagation with radial and axial wall motion. Since the Young wave is excited by pulsatile pressure and is examined in clinical studies, commonly measured pulsatile parameters in the Young wave are expressed in terms of pulsatile pressure and their values are calculated with the well-established values of circumferential elasticity (E_θ) and initial tension ($T_{\theta 0}$) and assumed values of axial elasticity (E_x) and initial tension (T_{x0}) at the ascending aorta and the carotid artery. The corresponding values with the exclusion of axial wall motion are also calculated. Comparison of the calculated results between inclusion and exclusion of axial wall motion indicates that (1) axial wall motion does not affect radial wall motion and other commonly measured pulsatile parameters, except wall shear stress; (2) axial wall motion is caused by wall shear stress and radial wall displacement gradient with a factor of ($T_{x0}-T_{\theta 0}$), and enables axial power transmission through the arterial wall; and (3) while radial wall motion reflects E_θ and $T_{\theta 0}$, axial wall motion reflects E_x and ($T_{x0}-T_{\theta 0}$). [DOI: 10.1115/1.4053863]

Keywords: arterial wall, orthotropic, elasticity, initial tension, radial motion, axial motion, pulse wave propagation, atherosclerosis

1 Introduction

Atherosclerosis alters arterial wall mechanical properties, thereby affecting pulse wave propagation in arteries and ultimately causing heart disease. In clinical studies, different pulsatile parameters at an artery are measured for the early detection of atherosclerosis [1–6]. To date, the majority of clinical measures are focused on the radial motion of the arterial wall and have shed great insights into its physiological implications. However, these clinical measures remain limited for the detection of subclinical atherosclerosis [1–6]. In recent years, the axial displacement amplitude of the arterial wall is found to be comparable with its radial displacement amplitude (e.g., 0.5 mm versus 0.6 mm at the carotid artery [4]) [1–6]. A recent clinical study finds that axial motion of the arterial wall is a more sensitive measure of subclinical atherosclerosis, and correlates with cardiovascular (CV) risk factors differently, as compared with radial-motion-based clinical measures [3]. Meanwhile, the studies on excised arteries find that axial initial tension in the arterial wall affects arterial wall remodeling and growth and plays an important role in vascular homeostasis [7,8]. Circumferential initial tension in the arterial wall is also found to affect the pulse wave propagation velocity [9]. Yet, in recent decades, the theories and related numerical models on arterial pulse wave propagation are focused on the governing equations of blood flow in an artery and include only radial motion of the arterial wall as a boundary condition, and thus are unsuitable to examine the axial motion and two initial tensions of the arterial wall for their role in arterial pulse wave propagation [10].

A long history exists on studying the problem of pulsatile blood flow in arteries. In the 1950–1960s, a large body of literature was established that examines this problem with radial and axial motion of the arterial wall [11–15]. Among them, Womersley [11] established the theoretical framework by treating blood flow as incompressible, Newtonian fluid, and the arterial wall as a thin-walled isotropic tube. Based on this framework, many other factors, including various tube models for the arterial wall [14], were considered for their influence on arterial pulse wave propagation. For instance, Atabek [12] treated the arterial wall as a thin-walled orthotropic tube and considered its two initial tensions, and Mirsky [13] treated the arterial wall as a thick-walled orthotropic tube but did not consider the two initial tensions. Note that all these theories on arterial pulse wave propagation assume that the arterial wall mechanical properties do not vary along its thickness. Axial displacement of the arterial wall was not measurable in vivo and was considered to be negligible at that time, as compared with its radial displacement [11–15]. Therefore, these theories did not pan out for clinical studies later on, and the theories considering the solely radial motion of the arterial wall have become dominant [10]. Meanwhile, various constitutive models of the arterial wall are also developed that consider three layers and different biological components (e.g., elastin and collegan) in the arterial wall along its thickness [16,17]. These constitutive models are aimed to examine the relation of mechanical function to biological function in the arterial wall. Given that clinical studies measure the arterial wall motion at one point along the wall thickness to represent the collective behavior of the arterial wall at an artery site [1–6], these constitutive models are unpractical for clinical application.

Contributed by the Applied Mechanics Division Technical Committee on Dynamics & Control of Structures & Systems (AMD-DCSS) of ASME for publication in the Journal of Engineering and Science in Medical Diagnostics and Therapy. Manuscript received December 5, 2021; final manuscript received February 4, 2022; published online March 8, 2022. Assoc. Editor: Shijia Zhao.

To reveal the role of axial wall motion and the two initial tensions in arterial pulse wave propagation with mathematical simplicity, we treat the arterial wall as an initially tensioned thin-walled orthotropic tube and thus adopt the theory developed by Atabek [12]. In Atabek's theory [12], a total of nine arterial wall mechanical properties are needed to define the contribution of the arterial wall to pulse wave propagation. Given that only four pulsatile parameters (i.e., pulsatile blood pressure, axial blood flow rate, radial wall motion, and axial wall motion) [1,2] are independent measurables at an artery in clinical studies, such a large number of wall properties make the theory unpractical for clinical application. The relation of wave velocity and wave transmission to Womersley number was examined under different assumed values of the nine wall properties, but the influence of axial wall motion on commonly measured pulsatile parameters at an artery was not studied, and pulsatile parameters enabled by axial wall motion were not explored either [12]. Three axial constraints were considered to reduce the unpractically large axial wall displacement, which is inconsistent with the well-accepted theory on radial wall motion [12]. As compared with Atabek's work [12], the original contributions of this study include: (1) we incorporate related clinical findings into the Atabek's theory and remove axial constraints from it so that only four arterial wall mechanical properties: elasticity and initial tension in the axial and circumferential directions, are needed to define the contribution of the arterial wall to pulse wave propagation; (2) axial elasticity is utilized to factor in axial constraints and adjust axial wall displacement, consistent with the circumferential elasticity for radial wall displacement; (3) with inclusion and exclusion of arterial wall motion, we derive theoretical expressions for wave velocity, commonly measured pulsatile parameters, and pulsatile parameters enabled by axial wall motion, and calculate their values at the ascending aorta (AA) and the carotid artery (CA); and (4) comparison of the calculated values at the two arteries between inclusion and exclusion of axial wall motion are conducted to reveal the role of axial wall motion and the two initial tensions and associated physiological implications.

2 Arterial Pulse Wave Propagation Theory With Radial and Axial Motion of the Arterial Wall in the Literature

This section presents the theory developed by Atabek [12]. The arterial wall is initially tensioned in the axial direction, due to its anatomy [7,8], and in the circumferential direction, due to diastolic blood pressure (DBP). As such, the arterial wall is modeled as an initially tensioned thin-walled orthotropic tube. As shown in Fig. 1(*a*), the arterial wall geometry includes the inner radius a at DBP and thickness h. The arterial wall has elasticity E_θ and initial tension per unit length $T_{\theta 0} = \text{DBP} \times a$ in the circumferential direction, and elasticity E_x and initial tension per unit length T_{x0} in the axial direction (x-axis). During the time t of a pulse cycle, the arterial wall at a fixed axial-position x undergoes radial and axial motion, and thus has two pulsatile parameters: radial displacement $\eta(x,t)$ and axial displacement $\xi(x,t)$. The blood flow in the artery is assumed to be an incompressible, Newtonian fluid, and has three pulsatile parameters: radial blood flow velocity $w(r,x,t)$, axial blood flow velocity $u(r,x,t)$, and pulsatile blood pressure $\Delta p(r,x,t)$, where the radial coordinate r varies within $r \in (0,a)$.

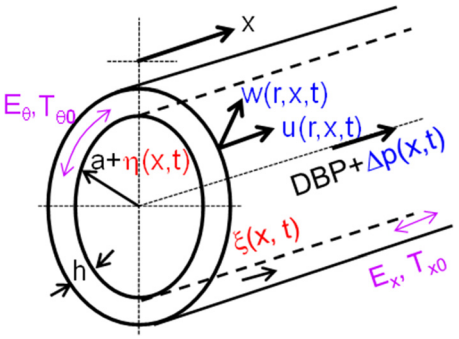

Fig. 1 Schematics of an artery: arterial wall geometries: inner radius *a* at DBP and thickness *h*; arterial wall mechanical properties: E_x, T_{x0}, E_θ, and $T_{\theta 0}$; three pulsatile parameters in blood flow: $w(r, x, t)$, $u(r, x, t)$, and $\Delta p(x, t)$; and two pulsatile parameters in the arterial wall: $\eta(x, t)$ and $\xi(x, t)$

Three fundamental assumptions for arterial pulse wave propagation [11–12] are that (1) The five pulsatile parameters are axisymmetric and small perturbations; (2) Change of the inner radius of the arterial wall is negligible during arterial wall motion so that the conditions and stresses at the blood-wall interface are calculated at $r = a$; and (3) The inner radius of the arterial wall is much smaller than the pulse wavelength λ ($a \ll \lambda$) and thus $\Delta p(r,x,t)$ is independent of r and becomes $\Delta p(x,t)$ [11,12].

The governing equations of blood flow in an artery include the continuity equation and the Navier–Stokes equations in the radial (r-axis) and axial (x-axis) directions [11]

$$\frac{\partial w}{\partial r} + \frac{w}{r} + \frac{\partial u}{\partial x} = 0 \tag{1a}$$

$$\rho_b \frac{\partial w}{\partial t} = -\frac{\partial \Delta p}{\partial r} + \mu\left(\frac{\partial^2 w}{\partial r^2} + \frac{1}{r}\frac{\partial w}{\partial r} - \frac{w}{r^2} + \frac{\partial^2 w}{\partial x^2}\right) \tag{1b}$$

$$\rho_b \frac{\partial u}{\partial t} = -\frac{\partial \Delta p}{\partial x} + \mu\left(\frac{\partial^2 u}{\partial r^2} + \frac{1}{r}\frac{\partial u}{\partial r} + \frac{\partial^2 u}{\partial x^2}\right) \tag{1c}$$

where ρ_b and μ denote the blood density and viscosity, respectively. The solution to Eq. (1) is the wave expressions for w, u, and Δp [11]

$$w = \left[-\Delta p_0 \frac{\beta_0^2 r}{2\mu\alpha_0^2} + B\frac{\beta_0}{\alpha_0 J_0(\alpha_0)} J_1(\alpha_0 r/a)\right] \cdot e^{i(\omega t - kx)} \tag{2a}$$

$$u = \left[-\Delta p_0 \frac{\beta_0 a}{\mu\alpha_0^2} + B\frac{J_0(\alpha_0 r/a)}{J_0(\alpha_0)}\right] \cdot e^{i(\omega t - kx)} \tag{2b}$$

$$\Delta p = \Delta p_0 \cdot e^{i(\omega t - kx)} \tag{2c}$$

where $\alpha_0^2 = i^3\alpha^2$ with $\alpha = a\sqrt{\rho_b \omega/\mu}$ being Womersley number and $\beta_0 = ia\omega/c = i\beta$ [11]; ω and k are the angular frequency of the heart rate and the wave number, respectively; and $k = \omega/c$, where c is the wave velocity.

The governing equations of the arterial wall for its radial and axial motion are [12]

$$\rho h \frac{\partial^2 \eta}{\partial t^2} = \left\{\Delta p - 2\mu \cdot \frac{\partial w}{\partial r}\right\}_{r=a} + T_{\theta 0} \cdot \frac{\eta}{a^2} + T_{x0} \cdot \frac{\partial^2 \eta}{\partial x^2} - \frac{E_\theta h}{1 - \upsilon_\theta \upsilon_x} \cdot \left\{\frac{\eta}{a^2} + \frac{\upsilon_x}{a} \cdot \frac{\partial \xi}{\partial x}\right\} \tag{3a}$$

$$(\rho h + M)\frac{\partial^2 \xi}{\partial t^2} + C\frac{\partial \xi}{\partial t} + K\xi = -\mu\left\{\frac{\partial u}{\partial r} + \frac{\partial w}{\partial x}\right\}_{r=a} + \frac{\gamma E_\theta h}{1 - \upsilon_\theta \upsilon_x} \cdot \left\{\frac{\partial^2 \xi}{\partial x^2} + \frac{\upsilon_\theta}{a} \cdot \frac{\partial \eta}{\partial x}\right\} + \frac{T_{x0} - T_{\theta 0}}{a} \cdot \frac{\partial \eta}{\partial x} \tag{3b}$$

where ρ, υ_θ, and υ_x denote the density, circumferential Poisson's ratio, and axial Poisson's ratio of the arterial wall, respectively; and $\gamma = E_x/E_\theta$. Representing the tethering effect of neighboring tissue outside the arterial wall, M, C, and K, are inertial, damping, and elastic constraints, respectively, in the axial direction. The first

term on the right side of Eq. (3*b*) is wall shear stress (wss) τ_w. No-slip conditions at the blood-wall interface demand the blood flow velocities be equal to the arterial wall velocities in the radial and axial directions at the blood-wall interface

$$w_{r=a} = \frac{\partial \eta}{\partial t} \tag{3c}$$

$$u_{r=a} = \frac{\partial \xi}{\partial t} \tag{3d}$$

In Eq. (3), there are nine mechanical properties of the arterial wall: E_θ, $T_{\theta 0}$, υ_θ, E_x, T_{x0}, υ_x, M, C, and K. Note that the wall density is not included here, since it is commonly assumed constant in clinical studies and has a negligible role in affecting arterial pulse wave propagation.

The wave expressions for η and ξ are

$$\eta = \eta_0 \cdot e^{i(\omega t - kx)} \tag{4a}$$

$$\xi = \xi_0 \cdot e^{i(\omega t - kx)} \tag{4b}$$

Four constant unknowns: Δp_0, B, η_0, and ξ_0, are involved in the five pulsatile parameters in Eqs. (2) and (4). Substituting Eqs. (2) and (4) into Eq. (3) leads to a 4×4 matrix equation with a vector of the four constant unknowns. A nonzero solution for the four constant unknowns demands that the determinant of the 4×4 matrix in the equation be equal to zero, leading to the frequency equation that determines wave velocity and wave transmission in the Young wave and the Lamb wave in an artery. Since the Young wave is excited by pulsatile pressure [15,18], the rest three constant unknowns are further expressed in terms of Δp_0, based on the 4×4 matrix equation [12]. With the neglect of M, C, and K, the axial wall displacement was found to be extremely large, as compared with the radial wall displacement. Thus, M, C, and K were included for reducing the axial wall displacement. With different assumed values of the nine wall properties, the relation of the wave velocity and wave transmission in the two waves versus the Womersley number was examined in Ref. [12].

3 Improved Arterial Pulse Wave Propagation Theory With Radial and Axial Motion of the Arterial Wall

3.1 The Governing Equations of the Arterial Wall Modified With Related Clinical Findings. Although in vitro studies found that the arterial wall may be considered incompressible [19], Poisson's ratio of the arterial wall is assumed to be zero in obtaining the value of E_θ in clinical studies [1–6]. The great similarity in the measured waveforms of $\Delta p(x,t)$ and $\eta(x,t)$ at an artery [10] might indicate that the contribution of $\upsilon_x \cdot \partial\xi/\partial x$ to $\eta(x,t)$ is negligible in Eq. (3*a*). Thus, it is reasonable to assume $\upsilon_x = 0$. As compared with the rest terms, the inertial term, the T_{x0}-associated term, and the $\partial w/\partial r$-associated term are small quantities, and then Eq. (2*a*) is reduced to

$$0 = \{\Delta p\}_{r=a} - (E_\theta h - T_{\theta 0}) \cdot \frac{\eta}{a^2} \tag{5}$$

Although neighboring tissue outside the arterial wall is present, no radial constraints are considered to represent its tethering effect on the radial wall displacement when the value of E_θ is derived from the measured Δp-η relation in clinical studies [1–6]. Thus, the value of E_θ factors in the tethering effect of neighboring tissue in the radial direction. Similarly, it is reasonable to factor the tethering effect of neighboring tissue on the axial direction in the value of E_x, which is consistent with E_θ for the radial wall displacement. By removing the axial constraints, Eq. (3*b*) is rewritten as

$$\rho h \frac{\partial^2 \xi}{\partial t^2} = \gamma E_\theta h \cdot \frac{\partial^2 \xi}{\partial x^2} - \tau_w + \frac{\gamma \upsilon_\theta + \tau_{x0} - \tau_{\theta 0}}{a} E_\theta h \cdot \frac{\partial \eta}{\partial x} \quad \text{with} \quad \tau_w = \mu \left\{ \frac{\partial u}{\partial r} + \frac{\partial w}{\partial x} \right\}_{r=a} \tag{6}$$

Note that τ_w and the $\partial\eta/\partial x$ term with a factor of $(\gamma\upsilon_\theta + \tau_{x0} - \tau_{\theta 0})$ are the two sources for $\xi(x,t)$. By adjusting the value of τ_{x0}, $\gamma\upsilon_\theta$ can be factored into $(\tau_{x0} - \tau_{\theta 0})$, without altering $\xi(x,t)$. Then, it is also assumed that $\upsilon_\theta = 0$ and Eq. (6) is reduced to

$$\rho h \frac{\partial^2 \xi}{\partial t^2} = \gamma E_\theta h \cdot \frac{\partial^2 \xi}{\partial x^2} - \tau_w + \frac{\tau_{x0} - \tau_{\theta 0}}{a} E_\theta h \cdot \frac{\partial \eta}{\partial x} \tag{7}$$

Based on Eqs. (5) and (7), only four arterial wall mechanical properties: E_θ, $T_{\theta 0}$, E_x, and T_{x0}, are needed to define the contribution of the arterial wall to arterial pulse wave propagation.

3.2 Solution. Substituting the wave expressions for the five pulsatile parameters into Eqs. (3*c*), (3*d*), (5), and (7) leads to the following 4×4 matrix equation with a vector of the four constant unknowns:

$$\begin{bmatrix} -\dfrac{\beta_0 a}{\mu \alpha_0^2} & 1 & 0 & -i\omega \\ -\dfrac{\beta_0^2 a}{2\mu\alpha_0^2} & \dfrac{1}{2}\beta_0 F_{10} & -i\omega & 0 \\ 1 & 0 & (\tau_{\theta 0} - 1)\dfrac{E_\theta h}{a^2} & 0 \\ -\dfrac{\beta_0^3}{2\alpha_0^2} & \dfrac{\mu\alpha_0^2}{2a} F_{10} & -(\tau_{x0} - \tau_{\theta 0})\dfrac{E_\theta h \beta_0}{a^2} & \dfrac{\gamma E_\theta h \beta_0^2}{a^2} + \rho h \omega^2 \end{bmatrix} \begin{Bmatrix} \Delta p_0 \\ B \\ \eta_0 \\ \xi_0 \end{Bmatrix} = \begin{Bmatrix} 0 \\ 0 \\ 0 \\ 0 \end{Bmatrix} \tag{8}$$

where

$$\tau_{\theta 0} = T_{\theta 0}/(E_\theta h), \quad \tau_{x0} = T_{x0}/(E_\theta h), \quad F_{10} = \frac{2J_1(\alpha_0)}{\alpha_0 J_0(\alpha_0)} \tag{9}$$

Note that τ_{x0} and $\tau_{\theta 0}$ are normalized initial tensions, and F_{10} is due to fluid-loading and takes complex values.

Assigning the determinant of the 4×4 matrix in Eq. (8) to zero gives rise to the frequency equation that determines wave velocities in an artery

$$\left\{F_{10}(2\tau_{x0}-\tau_{\theta 0}-1)-2(1-F_{10})(1-\tau_{\theta 0})K-4\gamma\right\}\frac{c_0^2}{c^2}$$
$$+4(1-F_{10})\cdot\left\{(1-\tau_{\theta 0})\gamma\right\}\frac{c_0^4}{c^4}+F_{10}+2K=0 \tag{10}$$

where

$$c_0=\sqrt{\frac{E_\theta h}{2\rho_b a}},\quad K=\frac{\rho h}{\rho_b a} \tag{11}$$

Equation (10) is a quadratic equation of c_0^2/c^2, indicating the existence of the two waves: The Young wave and Lamb wave [13–15]. The two roots of Eq. (10) correspond to the Young wave (c_1) and the Lamb wave (c_2). The wave velocity (or phase velocity) of the Young wave and the Lamb wave become real(c_1) and real(c_2), respectively. The wave transmission per wavelength is then calculated as $\exp(-2\pi Y/X)$, with $c=X+Yi$ (Note: X and Y take real values).

Removal of F_{10}, τ_{x0}, and $\tau_{\theta 0}$ in Eq. (8) separates the Young wave and the Lamb wave and leads to the wave velocities of uncoupled radial motion and axial motion of the arterial wall, respectively,

$$c_1=c_0=\sqrt{\frac{E_\theta h}{2\rho_b a}}=PWV\quad\text{(uncoupled Young wave)} \tag{12a}$$

$$c_2=\sqrt{\frac{E_x}{\rho}}=c_L\quad\text{(Uncoupled Lamb wave)} \tag{12b}$$

Note that c_1 is reduced to the Moens–Korteweg formula for pulse wave velocity (PWV), which is commonly used in clinical studies [1–6,10], and c_2 is reduced to longitudinal elastic wave velocity c_L [18].

3.3 Commonly Measured Pulsatile Parameters in the Young Wave. In clinical studies, all the measured pulsatile parameters are considered in the Young wave. Although the Lamb wave was measured on excised arteries [20], very little effort has been taken on measuring the Lamb wave in clinical studies. Therefore, only the Young wave is analyzed here. In terms of Δp_0, the rest three constant unknowns can be derived from Eq. (8)

$$\eta_0=\frac{a}{2c^2\rho_b}(1+mF_{10})\Delta p_0,\quad \xi_0=\frac{(1+m)}{i\omega c\rho_b}\Delta p_0,\quad B=\frac{m}{c\rho_b}\Delta p_0 \tag{13}$$

where

$$m=\frac{\dfrac{c^2}{c_0^2}+(\tau_{\theta 0}-1)}{(1-\tau_{\theta 0})F_{10}} \tag{14}$$

Note that Δp_0, η_0, and ξ_0 represent the amplitudes of pulsatile pressure, and radial displacement and axial displacement of the arterial wall, respectively.

In clinical studies, $\Delta p(x,t)$ and $\eta(x,t)$ are commonly measured for E_θ at an artery [1–6]. Additionally, blood flow rate $Q(x,t)$, axial power transmission through blood flow $P_{\text{blood}}(x,t)$, and wall shear stress $\tau_w(x,t)$ at an artery are also measured [10]. Their theoretical expressions in terms of $\Delta p(x,t)$ are derived

$$Q=\int_0^a u2\pi r dr=\frac{\pi a^2}{c\rho_b}(1+mF_{10})\cdot\Delta p \tag{15}$$

$$P_{\text{blood}}=\Delta p\cdot Q=\frac{\pi a^2}{c\rho_b}(1+mF_{10})\cdot\Delta p^2 \tag{16}$$

$$\tau_w=\frac{a\omega}{2c}\cdot imF_{10}\cdot\Delta p \tag{17}$$

3.4 Pulsatile Parameters Enabled by Axial Wall Motion in the Young Wave. Inclusion of $\xi(x,t)$ implies that wall shear stress $\tau_w(x,t)$ and the $\partial\eta/\partial x$ term with a factor of $(\tau_{x0}-\tau_{\theta 0})$ in Eq. (7) can transmit power $P_{\text{wss}}(x,t)$ and $P_{\text{tension}}(x,t)$, respectively, into the arterial wall

$$P_{\text{wss}}=\tau_{w0}2\pi a\dot{\xi}/(ik)=\left[\frac{\mu\omega}{\rho_b c^2}+imF_{10}\right]\cdot\frac{\pi a^2(1+m)}{ic\rho_b}\Delta p^2 \tag{18}$$

$$P_{\text{tension}}=-2\pi a\,(T_{x0}-T_{\theta 0})\frac{(1+mF_{10})}{2c^3{\rho_b}^2}(1+m)\Delta p^2 \tag{19}$$

Meanwhile, the inclusion of $\xi(x,t)$ also implies that there is axial power transmission $P_{\text{wall}}(x,t)$ through the arterial wall

$$P_{\text{wall}}=E_x\frac{\partial\xi}{\partial x}2\pi ah\dot{\xi}=-2\pi ahE_x\frac{(1+m)^2}{c^3{\rho_b}^2}\Delta p^2 \tag{20}$$

4 Arterial Pulse Wave Theory With Exclusion of Axial Wall Motion

To illustrate how the inclusion of $\xi(x,t)$ affects the Young wave, the theory on arterial pulse wave propagation with $\xi(x,t)=0$ is presented here for comparison.

4.1 Inclusion of Radial Fluid-Loading and Circumferential Initial Tension. With $\xi(x,t)=0$, the governing equation for $\eta(x,t)$ and the two no-slip conditions at the blood-wall interface become

$$0=\{\Delta p\}_{r=a}-(E_\theta h-T_{\theta 0})\cdot\frac{\eta}{a^2} \tag{21a}$$

$$w_{r=a}=\frac{\partial\eta}{\partial t} \tag{21b}$$

$$u_{r=a}=0 \tag{21c}$$

Equation (21b) represents radial fluid-loading. Since $\xi(x,t)$ is excluded, axial fluid-loading, τ_w in Eq. (7), is omitted. Exclusion of $\xi(x,t)$ does not vary the wave expressions for w, u, and Δp in Eq. (2). Substituting Eqs. (2) and (4a) into Eq. (21) leads to a 3×3 matrix equation with a vector of the three constant unknowns: Δp_0, B, and η_0:

$$\begin{bmatrix}-\dfrac{\beta_0 a}{\mu\alpha_0^2} & 1 & 0\\ -\dfrac{\beta_0^2 a}{2\mu\alpha_0^2} & \dfrac{1}{2}\beta_0 F_{10} & -i\omega\\ 1 & 0 & (\tau_{\theta 0}-1)\dfrac{E_\theta h}{a^2}\end{bmatrix}\begin{Bmatrix}\Delta p_0\\ B\\ \eta_0\end{Bmatrix}=\begin{Bmatrix}0\\0\\0\end{Bmatrix} \tag{22}$$

Assigning the determinant of the 3×3 matrix in Eq. (22) to zero provides the frequency equation

$$c^2=\frac{E_\theta h}{2\rho_b a}(1-F_{10})(1-\tau_{\theta 0}) \tag{23}$$

where F_{10} results from radial fluid-loading. Accordingly, there is only the Young wave with the wave velocity

$$c=c_0\sqrt{(1-F_{10})(1-\tau_{\theta 0})} \tag{24}$$

Table 1 Related values of the mechanical properties and geometries at the AA and the CA [13,21,22]

	Parameter	Symbol	CA	AA
Arterial wall	Pulsatile pressure amplitude	Δp_0	48 mmHg	40 mHg
	Radius	a	3.3 mm	13 mm
	Thickness	h	0.62 mm	2 mm
	Elasticity	E_θ	771 kPa	400 kPa
	Density	ρ	1055 kg/m^3	
Blood	Density	ρ_b	1055 kg/m^3	
	Viscosity	μ	0.004 Pa·s	

Exclusion of $\xi(x,t)$ eliminates the Lamb wave and leads to $m=-1$ in the expressions for η_0 and B in Eq. (13) and the expressions for $Q(x,t)$, $P_{\text{blood}}(x,t)$, and $\tau_w(x,t)$ in Eqs. (15)–(17).

4.2 Exclusion of Radial Fluid-Loading and Circumferential Initial Tension. When $w(x,t)$ in Eq. (1*b*), friction force in Eq. (1*c*), and $T_{\theta 0}$ in Eq. (21*a*) are all neglected, Eqs. (1*a*), (1*c*), and (21*a*) form the three governing equations for obtaining the Moens–Korteweg formula for PWV [3]

$$c = c_0 = \sqrt{\frac{E_\theta h}{2\rho_b a}} = PWV \tag{25}$$

Note that PWV has a real value, and the wave transmission becomes one. The expression for η_0 in Eq. (13) and the expressions for $Q(x,t)$ and $P_{\text{blood}}(x,t)$ in Eqs. (15) and (16) are still applicable with $mF_{10}=0$.

5 Results and Discussion

5.1 Calculated Results at the Ascending Aorta and the Carotid Artery. Attached to the left ventricle, the AA carries high physiological relevance to the left ventricle, but its clinical measurements are uncommon, due to difficult access [2]. The CA is the most commonly measured artery and carries higher clinical values [1–6]. Thus, we apply the developed theories in Secs. 3 and 4 to these two arteries to examine how the inclusion of $\xi(x,t)$ affects the Young wave. Table 1 summarizes the well-established values at the two arteries [13,21,22]. The value of E_θ is obtained with Poisson's ratio being assumed zero and neglect of $\xi(x,t)$. Note that $T_{\theta 0}=\text{DBP}\times a$ and $\tau_{\theta 0}$ is fixed at 0.1 at the two arteries [12]. Although many studies have recognized orthotropic elasticity in the arterial wall, the suggested values of E_x swing from being a fraction of E_θ [23] to being above E_θ [24]. Thus, we vary $\gamma=E_x/E_\theta$ at different values for its influence on the Young wave. Since the values of ξ_0 and η_0 at the CA are found to be comparable in clinical studies [1–6], γ is varied until achieving comparable values for them. Similarly, there are no well-accepted values on τ_{x0}. We assume $\tau_{x0}=0.1$ to examine the sole contribution of $\tau_w(x,t)$ to $\xi(x,t)$, and $\tau_x=0.2$ to examine the combined

Table 2 The influence of axial motion $\xi(x,t)$ on pulse wave propagation at the AA

(a) Wave velocity and transmission of the Young and Lamb waves

	Radial motion and axial motion						Radial motion only		
	$\tau_{\theta 0}=0.1$, $\tau_{x0}=0.1$			$\tau_{\theta 0}=0.1$, $\tau_{x0}=0.2$			$m=-1$		$mF_{10}=0$
	$\gamma=1/3$	$\gamma=1$	$\gamma=3$	$\gamma=1/3$	$\gamma=1$	$\gamma=3$	$\tau_{\theta 0}=0.1$	$\tau_{\theta 0}=0.0$	$\tau_{\theta 0}=0.0$
Real(c_1) (m/s)	4.93	4.93	4.93	4.97	4.94	4.93	4.93	5.20	5.400
Exp($-2\pi Y_1/X_1$)	0.7576	0.7748	0.7793	0.7944	0.7846	0.7824	0.7814	0.7814	1.0
Real (c_2) (m/s)	9.94	17.22	29.82	9.87	17.18	29.80	—	—	—
Exp($-2\pi Y_2/X_2$)	0.5715	0.5587	0.5555	0.5449	0.5517	0.5533	—	—	—

(b) Amplitudes of commonly measured pulsatile parameters in the Young wave

	Radial motion and axial motion						Radial motion only		
	$\tau_{\theta 0}=0.1$, $\tau_{x0}=0.1$			$\tau_{\theta 0}=0.1$, $\tau_{x0}=0.2$			$m=-1$		$mF_{10}=0$
	$\gamma=1/3$	$\gamma=1$	$\gamma=3$	$\gamma=1/3$	$\gamma=1$	$\gamma=3$	$\tau_{\theta 0}=0.1$	$\tau_{\theta 0}=0.0$	$\tau_{\theta 0}=0.0$
η_0 (mm)	1.252	1.252	1.252	1.252	1.252	1.252	1.252	1.127	1.127
Q (m^3/s)	5.04×10^{-4}	5.04×10^{-4}	5.04×10^{-4}	5.08×10^{-4}	5.05×10^{-4}	5.05×10^{-4}	5.04×10^{-4}	4.79×10^{-4}	4.97×10^{-4}
P_{blood} (watt)	2.690	2.690	2.690	2.710	2.695	2.692	2.690	2.552	2.649
τ_ω (Pa)	6.178	5.895	5.822	5.064	5.592	5.727	5.789	5.492	0

(c) Amplitudes of pulsatile parameters related to axial motion in the Young wave

	Radial motion and axial motion					
	$\tau_{\theta 0}=0.1$, $\tau_{x0}=0.1$			$\tau_{\theta 0}=0.1$, $\tau_{x0}=0.2$		
	$\gamma=1/3$	$\gamma=1$	$\gamma=3$	$\gamma=1/3$	$\gamma=1$	$\gamma=3$
τ_ω (Pa)	6.178	5.895	5.822	5.064	5.592	5.727
The $\partial\eta/\partial x$ term (Pa)	0.00	0.00	0.00	12.173	12.238	12.255
P_{wss} (Pa)	2.81×10^{-2}	7.38×10^{-3}	2.29×10^{-3}	3.67×10^{-2}	1.10×10^{-2}	3.53×10^{-3}
P_{tension} (Pa)	0.00	0.00	0.00	8.82×10^{-2}	2.40×10^{-2}	7.54×10^{-3}
P_{wall} (watt)	3.48×10^{-2}	7.88×10^{-3}	2.34×10^{-3}	8.61×10^{-2}	1.92×10^{-2}	5.71×10^{-3}
ξ_0 (mm)	11.307	3.106	0.978	17.842	4.857	1.527
Ratio of η_0/ξ_0	0.111	0.403	1.280	0.070	0.258	0.820

Table 3 The influence of axial motion $\xi(x, t)$ on pulse wave propagation at the CA

(a) Wave velocity and transmission of the Young and Lamb waves

	Radial motion and axial motion								Radinal motion only		
	$\tau_{\theta 0}=0.1, \tau_{x0}=0.1$				$\tau_{\theta 0}=0.1, \tau_{x0}=0.2$				$m=-1$		$mF_{10}=0$
	$\gamma=1/3$	$\gamma=1$	$\gamma=3$	$\gamma=20$	$\gamma=1/3$	$\gamma=1$	$\gamma=3$	$\gamma=20$	$\tau_{\theta 0}=0.1$	$\tau_{\theta 0}=0.0$	$\tau_{\theta 0}=0.0$
Real (c_1) (m/s)	6.43	6.64	6.67	6.68	6.72	6.70	6.69	6.68	6.68	7.04	8.29
Transmission	0.2069	0.2950	0.3215	0.3322	0.2347	0.3084	0.3261	0.3329	0.3340	0.3340	1.0
Real (c_2) (m/s)	11.48	19.35	33.34	85.94	11.00	19.16	33.25	85.91	—	—	—
Transmission	0.5125	0.3633	0.3335	0.3228	0.4541	0.3476	0.3288	0.3221	—	—	—

(b) Amplitudes of commonly measured pulsatile parameters in the Young wave

	Radial motion and axial motion								Radial motion only		
	$\tau_{\theta 0}=0.1, \tau_{x0}=0.1$				$\tau_{\theta 0}=0.1, \tau_{x0}=0.2$				$m=-1$		$mF_{10}=0$
	$\gamma=1/3$	$\gamma=1$	$\gamma=3$	$\gamma=20$	$\gamma=1/3$	$\gamma=1$	$\gamma=3$	$\gamma=20$	$\tau_{\theta 0}=0.1$	$\tau_{\theta 0}=0.0$	$\tau_{\theta 0}=0.0$
η_0 (m)	0.162	0.162	0.162	0.162	0.162	0.162	0.162	0.162	0.162	0.146	0.146
Q (m^3/s)	2.23×10^{-5}	2.27×10^{-5}	2.28×10^{-5}	2.28×10^{-5}	2.32×10^{-5}	2.29×10^{-5}	2.28×10^{-5}	2.28×10^{-5}	2.28×10^{-5}	2.16×10^{-5}	2.50×10^{-5}
P_{blood} (watt)	0.142	0.145	0.146	0.146	0.148	0.147	0.146	0.146	0.146	0.138	0.160
τ_ω (Pa)	6.282	5.140	4.891	4.799	5.492	4.913	4.821	4.789	4.783	4.538	0

(c) Amplitudes of pulsatile parameters related to axial motion in the Young wave

	Radial motion and axial motion							
	$\tau_{\theta 0}=0.1, \tau_{x0}=0.1$				$\tau_{\theta 0}=0.1, \tau_{x0}=0.2$			
	$\gamma=1/3$	$\gamma=1$	$\gamma=3$	$\gamma=20$	$\gamma=1/3$	$\gamma=1$	$\gamma=3$	$\gamma=20$
τ_ω (Pa)	6.282	5.140	4.891	4.799	5.492	4.913	4.821	4.789
The $\partial\eta/\partial x$ term (Pa)	0	0	0	0	2.672	2.703	2.712	2.716
P_{wss} (Pa)	2.87×10^{-2}	6.09×10^{-3}	1.78×10^{-3}	2.54×10^{-4}	1.92×10^{-2}	4.00×10^{-3}	1.19×10^{-3}	1.71×10^{-4}
P_{tension} (Pa)	0	0	0	0	9.34×10^{-3}	2.20×10^{-3}	6.69×10^{-4}	9.68×10^{-5}
P_{wall} (watt)	3.39×10^{-2}	6.46×10^{-3}	1.82×10^{-3}	2.54×10^{-4}	1.76×10^{-2}	2.98×10^{-3}	8.28×10^{-4}	1.16×10^{-4}
ξ_0 (mm)	33.198	8.452	2.590	0.376	24.429	5.762	1.751	0.253
Ratio of η_0/ξ_0	0.005	0.019	0.063	0.431	0.007	0.028	0.093	0.640

Table 4 The influence of axial motion $\xi(x, t)$ on pulse wave propagation at the AA with the increased blood viscosity 0.006 Pa·s

(a) Wave velocity and transmission of the Young and Lamb waves

	Radial motion and axial motion					
	$\tau_{\theta 0}=0.1$, $\tau_{x0}=0.1$			$\tau_{\theta 0}=0.1$, $\tau_{x0}=0.2$		
	$\gamma=1/3$	$\gamma=1$	$\gamma=3$	$\gamma=1/3$	$\gamma=1$	$\gamma=3$
Real(c_1) (m/s)	4.88	4.89	4.89	4.93	4.90	4.89
Exp($-2\pi Y_1/X_1$)	0.7039	0.7280	0.7344	0.7461	0.7393	0.7379
Real(c_2) (m/s)	9.69	16.78	29.05	9.59	16.73	29.02
Exp($-2\pi Y_2/X_2$)	0.5286	0.5109	0.5065	0.4984	0.5031	0.5041

(b) Amplitudes of commonly measured pulsatile parameters in the Young wave

	Radial motion and axial motion					
	$\tau_{\theta 0}=0.1$, $\tau_{x0}=0.1$			$\tau_{\theta 0}=0.1$, $\tau_{x0}=0.2$		
	$\gamma=1/3$	$\gamma=1$	$\gamma=3$	$\gamma=1/3$	$\gamma=1$	$\gamma=3$
η_0 (mm)	1.252	1.252	1.252	1.252	1.252	1.252
Q (m^3/s)	5.00×10^{-4}	5.00×10^{-4}	5.00×10^{-4}	5.05×10^{-4}	5.01×10^{-4}	5.01×10^{-4}
P_{blood} (watt)	2.667	2.667	2.667	2.691	2.674	2.669
τ_ω (Pa)	7.714	7.281	7.170	6.340	6.910	7.054

(c) Amplitudes of pulsatile parameters related to axial motion in the Young wave

	Radial motion and axial motion					
	$\tau_{\theta 0}=0.1$, $\tau_{x0}=0.1$			$\tau_{\theta 0}=0.1$, $\tau_{x0}=0.2$		
	$\gamma=1/3$	$\gamma=1$	$\gamma=3$	$\gamma=1/3$	$\gamma=1$	$\gamma=3$
τ_ω (Pa)	7.714	7.281	7.170	6.340	6.910	7.054
The $\partial\eta/\partial x$ term (Pa)	0	0	0	12.256	12.337	12.357
P_{wss} (Pa)	4.26×10^{-2}	1.10×10^{-2}	3.39×10^{-3}	4.39×10^{-2}	1.28×10^{-2}	4.10×10^{-3}
P_{tension} (Pa)	0	0	0	8.49×10^{-2}	2.29×10^{-2}	7.17×10^{-3}
P_{wall} (watt)	5.24×10^{-2}	1.17×10^{-2}	3.46×10^{-3}	8.03×10^{-2}	1.76×10^{-2}	5.21×10^{-3}
ξ_0 (mm)	13.814	3.767	1.184	17.173	4.629	1.452
Ratio of η_0/ξ_0	0.091	0.332	1.057	0.073	0.270	0.862

contribution of $\tau_w(x,t)$ and the $\partial\eta/\partial x$ term with a factor of $(\tau_{x0}-\tau_{\theta 0})$ to $\xi(x,t)$. The heart rate used in the calculation is 75 beats per minute (bpm).

Table 2 summarizes the calculated results at the AA. As shown in Table 2(*a*), when only $\eta(x,t)$ is considered, the inclusion of radial fluid-loading reduces the wave velocity and wave transmission in the Young wave; $\tau_{\theta 0}=0.1$ (or DBP) further reduces the wave velocity but does not affect the Young wave transmission. Inclusion of $\xi(x,t)$ does not affect the wave velocity and transmission in the Young wave at different values of E_x and τ_{x0}, but causes the Lamb wave. The Lamb wave velocity increases with E_x, but does not vary with τ_{x0}. The Lamb wave transmission does not vary with either E_x or τ_{x0}. While the Lamb wave velocity is higher than the Young wave velocity, the Lamb wave transmission is lower than the Young wave transmission.

As shown in Table 2(*b*), when only $\eta(x,t)$ is considered, the inclusion of radial fluid-loading does not affect η_0, but reduces Q and P_{blood}; $\tau_{\theta 0}=0.1$ increases η_0, Q, P_{blood}, and τ_ω. Inclusion of $\xi(x,t)$ does not affect η_0, Q, and P_{blood}. When $\gamma=1/3$, τ_ω is relatively high and decreases with τ_{x0}. In contrast, when $\gamma\geq 1$, the influence of $\xi(x,t)$ on τ_ω is largely negligible, at the two values of τ_{x0}. As shown in Table 2(*c*), the inclusion of $\xi(x,t)$ allows τ_ω and the $\partial\eta/\partial x$ term in Eq. (7) to transmit power into the arterial wall. When $(\tau_{x0}-\tau_{\theta 0})=0$, the $\partial\eta/\partial x$ term becomes zero and P_{wall} is very close to P_{wss}. When $(\tau_{x0}-\tau_{\theta 0})\neq 0$, the $\partial\eta/\partial x$ term is not zero, but P_{wall} is not simply a sum of P_{wss} and P_{tension}, due to a phase shift between them. ξ_0 decreases with E_x but increases with τ_{x0}. Similarly, P_{wall}, P_{wss}, and P_{tension} all decrease with E_x but increase with τ_{x0}. When $\gamma=3$, η_0 and ξ_0 are comparable at $\tau_{x0}=0.1$ and 0.2.

Table 3 summarizes the calculated results at the CA. As shown in Table 3(*a*), when only $\eta(x,t)$ is considered, the inclusion of radial fluid-loading reduces the wave velocity and wave transmission in the Young wave; $\tau_{\theta 0}=0.1$ (or DBP) further reduces the wave velocity but does not affect the wave transmission in the Young wave. The influence of $\xi(x,t)$ on the Young wave velocity is overall negligible, at different values of E_x and τ_{x0}. The influence of $\xi(x,t)$ on the Young wave transmission depends on γ. When $\gamma=1/3$, the inclusion of $\xi(x,t)$ greatly reduces the Young wave transmission. However, when $\gamma\geq 1$, the inclusion of $\xi(x,t)$ does not affect the Young wave transmission. While the Lamb wave velocity increases with E_x, but does not vary with τ_{x0}. When $\gamma\geq 1$, the Lamb wave transmission does not vary with either E_x or τ_{x0}. The Lamb wave transmission is much higher at $\gamma=1/3$ than that at $\gamma\geq 1$, but the influence of τ_{x0} on the Lamb wave transmission is largely negligible.

As shown in Table 3(*b*), when only $\eta(x,t)$ is considered, the inclusion of radial fluid-loading does not affect η_0, but reduces Q and P_{blood}; $\tau_{\theta 0}=0.1$ improves η_0, Q, and P_{blood}. Inclusion of $\xi(x,t)$ does not affect η_0, Q, and P_{blood}. When $\gamma=1/3$, the inclusion of $\xi(x,t)$ increases τ_ω but τ_ω decreases with τ_{x0}. When $\gamma\geq 1$, the inclusion of $\xi(x,t)$ does not affect τ_ω much. As shown in Table 3(*c*), when $(\tau_{x0}-\tau_{\theta 0})=0$, P_{wall} is very close to P_{wss}. When $(\tau_{x0}-\tau_{\theta 0})\neq 0$, the $\partial\eta/\partial x$ term is nonzero, P_{wall} is not simply the

Table 5 The influence of axial motion $\xi(x, t)$ on pulse wave propagation at the CA with the increased blood viscosity 0.006 Pa·s

(a) Wave velocity and transmission of the Young and Lamb waves

	Radial motion and axial motion							
	$\tau_{\theta 0}=0.1$, $\tau_{x0}=0.1$				$\tau_{\theta 0}=0.1$, $\tau_{x0}=0.2$			
	$\gamma=1/3$	$\gamma=1$	$\gamma=3$	$\gamma=20$	$\gamma=1/3$	$\gamma=1$	$\gamma=3$	$\gamma=20$
real(c_1) (m/s)	5.95	6.32	6.38	6.40	6.27	6.40	6.41	6.41
Transmission	0.1245	0.2014	0.2290	0.2404	0.1373	0.2121	0.2329	0.2410
Real(c_2) (m/s)	11.13	18.38	31.56	81.23	10.61	18.15	31.44	81.19
Transmission	0.5568	0.3549	0.3133	0.2986	0.5092	0.3376	0.3081	0.2979

(b) Amplitudes of commonly measured pulsatile parameters in the Young wave

	Radial motion and axial motion							
	$\tau_{\theta 0}=0.1$, $\tau_{x0}=0.1$				$\tau_{\theta 0}=0.1$, $\tau_{x0}=0.2$			
	$\gamma=1/3$	$\gamma=1$	$\gamma=3$	$\gamma=20$	$\gamma=1/3$	$\gamma=1$	$\gamma=3$	$\gamma=20$
η_0 (m)	0.162	0.162	0.162	0.162	0.162	0.162	0.162	0.162
Q (m^3/s)	2.11×10^{-5}	2.19×10^{-5}	2.20×10^{-5}	2.21×10^{-5}	2.21×10^{-5}	2.22×10^{-5}	2.21×10^{-5}	2.21×10^{-5}
P_{blood} (watt)	0.135	0.140	0.141	0.141	0.141	0.142	0.141	0.141
τ_ω (Pa)	8.195	6.550	6.168	6.028	7.407	6.280	6.084	6.016

(c) Amplitudes of pulsatile parameters related to axial motion in the Young wave

	Radial motion and axial motion							
	$\tau_{\theta 0}=0.1$, $\tau_{x0}=0.1$				$\tau_{\theta 0}=0.1$, $\tau_{x0}=0.2$			
	$\gamma=1/3$	$\gamma=1$	$\gamma=3$	$\gamma=20$	$\gamma=1/3$	$\gamma=1$	$\gamma=3$	$\gamma=20$
τ_ω (Pa)	8.195	6.550	6.168	6.028	7.41	6.280	6.084	6.016
The $\partial\eta/\partial x$ term (Pa)	0.000	0.000	0.000	0.000	2.804	2.795	2.803	2.805
P_{wss} (Pa)	3.99×10^{-2}	8.82×10^{-3}	2.56×10^{-3}	3.63×10^{-4}	2.93×10^{-2}	6.09×10^{-3}	1.78×10^{-3}	2.54×10^{-4}
P_{tension} (Pa)	0.000	0.000	0.000	0.000	1.11×10^{-2}	2.71×10^{-3}	8.21×10^{-4}	1.19×10^{-4}
P_{wall} (watt)	4.56×10^{-2}	9.29×10^{-3}	2.60×10^{-3}	3.64×10^{-4}	2.62×10^{-2}	4.66×10^{-3}	1.29×10^{-3}	1.79×10^{-4}
ξ_0 (mm)	37.466	9.953	3.051	0.442	29.075	7.090	2.150	0.311
Ratio of η_0/ξ_0	0.004	0.016	0.053	0.366	0.0056	0.0229	0.0754	0.5218

sum of P_{wss} and P_{tension}. ξ_0 decreases with both E_x and τ_{x0}. Similarly, P_{wall}, P_{wss}, and P_{tension} all decrease with both E_x and τ_{x0}. When $\gamma=20$, η_0 and ξ_0 are comparable at $\tau_{x0}=0.1$ and 0.2.

5.2 Comparison Between the Ascending Aorta and the Carotid Artery. Comparison of Tables 2(*a*) and 3(*a*) shows that the Young wave velocity increases from the AA to the CA, mainly due to the increasing E_θ, since the ratio of h/a does not vary much between the two arteries. Similarly, the Lamb wave velocity also increases from the AA to the CA, at the same value of γ. As expected, the Young wave transmission and the Lamb wave transmission at the AA are much higher than that at the CA, simply due to the large size of the AA. It is interesting to note that the Young wave transmission is much higher than the Lamb wave transmission at the AA, but the Young wave transmission and the Lamb wave transmission become comparable at the CA.

Although η_0, Q, and P_{blood} at the AA are much larger than their counterparts at the CA, the values (a few Pa) of τ_w at the two arteries are similar and the values (~40 kPa) of circumferential stress $\sigma_{\theta\theta}=E_\theta\cdot\eta_0/a$ at the two arteries are also similar. Interestingly, when η_0 and ξ_0 have comparable values at each artery, the values of axial stress $\sigma_{xx}=E_x\cdot\partial\xi/\partial x$ at the two arteries are both about a few kPa.

In vitro studies have found that E_x and T_{x0} vary at different arteries [23], but the in vivo values of E_x and T_{x0} at the two arteries are unclear. Clinical studies have found that η_0 and ξ_0 are comparable at the CA [1–6], but how ξ_0 is compared with η_0 at the AA is unknown yet. To achieve comparable η_0 and ξ_0, E_x needs to be 3 times and 20 times of E_θ at the AA and the CA, respectively, at the assumed values of τ_{x0}. When η_0 and ξ_0 are comparable, P_{blood} is about three orders of magnitude higher than P_{wall} at the two arteries. Thus, blood flow is the dominant medium carrier of axial power transmission at the two arteries.

5.3 Influence of Blood Viscosity. To examine how blood viscosity affects arterial pulse wave propagation, blood viscosity is increased from 0.004 Pa·s to 0.006 Pa·s and the calculated results at the two arteries are summarized in Tables 4 and 5. At the AA, the increased blood viscosity does not affect the wave velocity in both waves, but moderately reduces the wave transmission in both waves. At the CA, the increased blood viscosity does not affect the wave velocity in both waves, either. However, the increased blood viscosity reduces the Young wave transmission at the CA to a larger extent than at the AA and does not affect the Lamb wave transmission much.

At the AA, the increased blood viscosity does not affect η_0, Q, and P_{blood}. At the CA, the increased blood viscosity does not affect η_0, but affects Q and P_{blood} to some extent. τ_ω is noticeably increased by the increased blood viscosity at the two arteries, with τ_ω being increased at the CA to a larger extent than at the AA. When $(\tau_{x0}-\tau_{\theta 0})=0$, only τ_ω contributes to ξ_0, with the latter being also increased at the two arteries. Accordingly, both P_{wss}

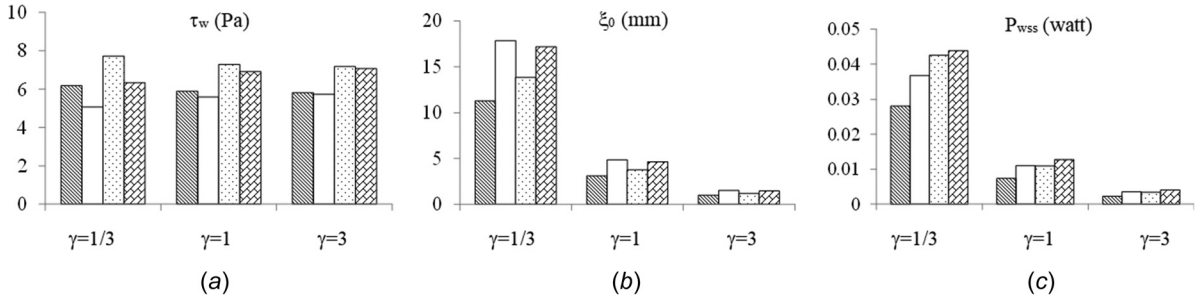

Fig. 2 Comparison of (*a*) wall shear stress (*b*) axial displacement (*c*) power transmitted into the arterial wall by wall shear stress at the AA under different values of γ, initial tensions, and blood viscosity (legends: $\tau_{\theta 0} = \tau_{x0} = 0.1$, $\mu = 0.004$ Pa·s, $\tau_{\theta 0} = 0.1$, $\tau_{x0} = 0.2$, $\mu = 0.004$ Pa·s, $\tau_{\theta 0} = \tau_{x0} = 0.1$, $\mu = 0.006$ Pa·s, $\tau_{\theta 0} = 0.1$, $\tau_{x0} = 0.2$, $\mu = 0.006$ Pa·s)

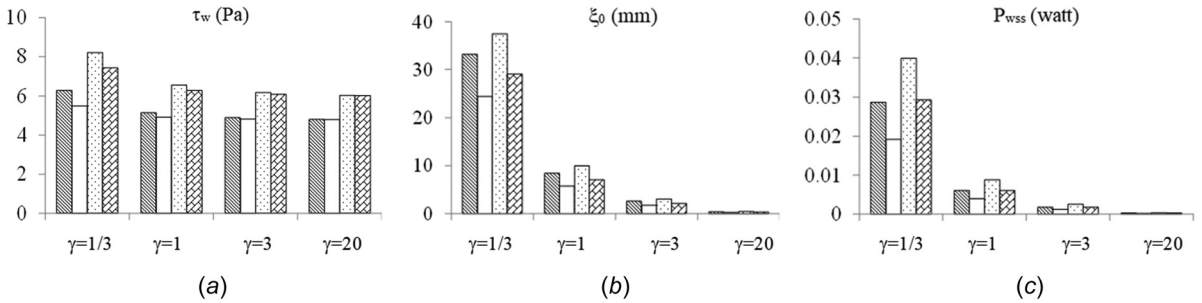

Fig. 3 Comparison of (*a*) wall shear stress (*b*) axial displacement (*c*) power transmitted into the arterial wall by wall shear stress at the CA under different values of γ, initial tensions, and blood viscosity (legends: $\tau_{\theta 0} = \tau_{x0} = 0.1$, $\mu = 0.004$ Pa·s, $\tau_{\theta 0} = 0.1$, $\tau_{x0} = 0.2$, $\mu = 0.004$ Pa·s, $\tau_{\theta 0} = \tau_{x0} = 0.1$, $\mu = 0.006$ Pa·s, $\tau_{\theta 0} = 0.1$, $\tau_{x0} = 0.2$, $\mu = 0.006$ Pa·s)

and P_{wall} are also increased. When $(\tau_{x0} - \tau_{\theta 0}) \neq 0$, the $\partial\eta/\partial x$ term is not zero. Due to a phase shift between them, the $\partial\eta/\partial x$ term and τ_ω contribute differently to ξ_0. At the value of $(\tau_{x0} - \tau_{\theta 0}) = 0.2$, the increased blood viscosity does not affect ξ_0 and P_{wall} at the AA but increases ξ_0 and P_{wall} at the CA.

As shown in Tables 2–5, since the Young wave velocity, η_0, Q, and P_{blood} are not affected much by the inclusion of $\xi(x,t)$, at the considered values of γ and $\tau_{\theta 0}$, no graphs are plotted for their dependence on γ and $\tau_{\theta 0}$. Since τ_ω, ξ_0, and P_{wss} are directly associated with $\xi(x,t)$ and are also affected by γ and $\tau_{\theta 0}$, the dependence of τ_ω, ξ_0, and P_{wall} on γ, $\tau_{\theta 0}$, and blood viscosity at the AA and the CA are plotted in Figs. 2 and 3, respectively. At the two arteries, when $\gamma = 1/3$, $\tau_{\theta 0}$ has a greater influence on τ_ω, ξ_0, and P_{wall}, but when $\gamma \geq 1$, the influence of $\tau_{\theta 0}$ on them becomes slight. While τ_ω is not affected much by γ, ξ_0 and P_{wall} are greatly reduced by increased γ. Overall, increased blood viscosity increases τ_ω, ξ_0, and P_{wall}.

5.4 Role of Axial Wall Motion and Two Initial Tensions. While the Young wave is excited by pulsatile pressure in blood flow, the Lamb wave is excited by the axial wall [15,18]. Whether ξ, τ_ω, and P_{wall} in the Lamb wave are comparable to their counterparts in the Young wave is unclear. It is known that $\eta, \Delta p, Q$, and P_{blood} in the Lamb wave are negligible, as compared with their counterparts in the Young wave [15,18]. As such, these four commonly measured pulsatile parameters are considered to be solely in the Young wave. The calculated results indicate that $\eta(x,t)$ reflects two properties: E_θ and $T_{\theta 0}$, and is not affected by $\xi(x,t)$. since Q and P_{blood} are closely related to $\eta(x,t)$, they are not affected by $\xi(x,t)$ much. This validates that clinical studies can interpret these pulsatile parameters with the arterial pulse wave propagation theory with the exclusion of $\xi(x,t)$. Additionally, $T_{\theta 0}$ (or DBP) has the effect of reducing the wave velocity. This explains the influence of DBP on PWV observed in clinical studies [8].

The calculated results reveal that $\xi(x,t)$ reflects axial elasticity E_x and the difference in initial tension: $(T_{x0} - T_{\theta 0})$. Thus, $\xi(x,t)$ and $\eta(x,t)$ reflect different mechanical properties of the arterial wall. This might explain the reason that $\xi(x,t)$ and $\eta(x,t)$ is correlated with CV risk factors differently [3]. $\xi(x,t)$ is found to be a more sensitive measure of subclinical atherosclerosis [3], as compared with $\eta(x,t)$, possibly indicating that subclinical atherosclerosis affects E_x and T_{x0} to a larger extent than E_θ and $T_{\theta 0}$. Given intersubject variations of atherosclerosis and concomitant-changing nature of various pulsatile parameters in the CV system [1–6], simultaneous examination of radial motion and axial motion of the arterial wall may provide a comprehensive assessment of the arterial wall and improve accuracy in the detection of subclinical atherosclerosis.

In the Young wave, when E_x is well below E_θ, τ_ω is affected by the inclusion of $\xi(x,t)$; when E_x is equal to or well above E_θ, inclusion of $\xi(x,t)$ does not affect τ_ω. Most importantly, the inclusion of $\xi(x,t)$ allows τ_ω and the $\partial\eta/\partial x$ term to transmit power into the arterial wall, and consequently, there is axial power transmission P_{wall} through the arterial wall. Here, it should be emphasized that although blood flow is the medium carrier of P_{blood}, $\eta(x,t)$ in the arterial wall dictates the value of P_{blood}, given that wave velocity c in Eq. (16) is determined by E_θ and $T_{\theta 0}$. As such, E_θ and $T_{\theta 0}$ dictate P_{blood}, and E_x and $(T_{x0} - T_{\theta 0})$ dictate P_{wall}.

The arterial wall contains two primary types of cells: endothelium cells (EC) and smooth muscle cells (SMC). EC and SMC respond to changes in their local mechanical loading and play an important role in maintaining vascular homeostasis [8]. Despite being much smaller than Δp ($\sim$ a few kPa), τ_ω ($\sim$ a few Pa) is an important determinant of EC functions [8]. Meanwhile, τ_ω affects the axial wall displacement and thus the axial strain in the arterial wall, which is found to also play a role in vascular homeostasis [8]. Similarly, although P_{wall} enabled by $\xi(x,t)$ is well below P_{blood}, EC and SMC are subjected to $\xi(x,t)$ and P_{wall}, which might affect EC and SMC functions [7,8].

The AA and the CA both have a tapered geometry along their length. Since the inclusion of $\xi(x,t)$ does not affect the Young wave velocity, Eq. (23) is rewritten here to examine how their tapered geometry affects the Young wave velocity

$$c = \sqrt{\frac{E_\theta h}{2\rho_b}(1-\tau_{\theta 0})\frac{1-F_{10}}{a}} \tag{26}$$

Note that F_{10} is a function of a. If E_θ, h, ρ_b, and $\tau_{\theta 0}$ are assumed to be the same along the artery length, and a is assumed to reduce by 20% from the entrance to the end of each artery, the Young wave velocity is increased by 10% and 6.7%, respectively, at the AA and the CA. A high Young wave velocity also translates to high wave reflection [1–6]. As such, the tapered geometry of an artery increases the Young wave velocity and causes higher wave reflection at the artery. These two conclusions are consistent with the related numerical findings with no inclusion of $\xi(x,t)$ in the literature [25]. Furthermore, the tapered geometry of an artery reduces η_0, Q, and P_{blood}, but increases τ_ω and ξ_0, as compared with their counterparts at the entrance of an artery. Evidently, the discussion on the tapered geometry of an artery here is rather simplified, without considering the continuity of all the parameters from the entrance to the end of an artery [25].

The two load-bearing components in the arterial wall are elastin and collagen, whose orientations affect the anisotropic mechanical properties of the arterial wall [26,27]. As such, the arterial wall is anisotropic in nature. In reality, the displacement of the arterial wall can be divided into three directions: axial, circumferential, and radial. As such, axial, circumferential, and radial elasticities are collective anisotropic properties of the arterial wall to capture the relations of displacement versus force in each of the three directions, respectively. Since the arterial wall is treated as a thin-walled tube in this study, its radial elasticity and radial displacement are neglected. To account for the radial elasticity of the arterial wall, the arterial wall needs to be treated as a thick-walled tube and its radial displacement can then be added to the governing equations of the arterial wall [13]. How the inclusion of radial elasticity affects pulse wave propagation is found to depend heavily on the assumed values of the three elasticities and their associated Poisson's ratios [13].

5.5 Study Limitations. There are four major limitations to this study. The developed theory represents free wave propagation in an infinitely long tube. As such, one limitation is that wave reflection is not considered in the study. It is known that wave reflection may increase or decrease the amplitudes of different pulsatile parameters to some extent [10,25]. Second, a pulsatile parameter is a sum of the fundamental and higher harmonic components with different amplitudes and phase angles [13,28]. This study considers only the fundamental component. While the amplitudes of η, Q, and P_{blood} are not directly varied with ω, the amplitudes of ξ and τ_w directly vary with ω. Third, the ratio of h/a is 0.15 and 0.19 at the AA and the CA, respectively. Strictly speaking, the two arteries should be treated as a thick-walled tube [13]. Finally, this study does not consider ξ, τ_ω, and P_{wall} in the Lamb wave. Nevertheless, these limitations are not expected to alter the role of $\xi(x,t)$ and two initial tensions in the Young wave revealed in this study.

6 Conclusion

By modeling the arterial wall as an initially tensioned thin-walled orthotropic tube and modifying the governing equations of the arterial wall with related clinical findings, a theoretical study is conducted on arterial pulse wave propagation with radial and axial motion of the arterial wall. In terms of pulsatile pressure, theoretical expressions are derived for commonly measured pulsatile parameters and pulsatile parameters enabled by axial wall motion in the Young wave. Comparison of the calculated values of wave velocity and these pulsatile parameters between inclusion and exclusion of axial wall motion at the AA and the CA reveals the following role of axial wall motion and the two initial tensions in the Young wave:

(1) Circumferential initial tension (or DBP) reduces the wave velocity but does not affect the wave transmission.
(2) Inclusion of axial wall motion does not affect radial wall motion, blood flow rate, and axial power transmission through blood flow.
(3) Depending on the value of $\gamma = E_x/E_\theta$, wall shear stress might be affected by the inclusion of axial wall motion.
(4) Axial wall motion is caused by wall shear stress and the $\partial\eta/\partial x$ term with a factor of $(\tau_{x0}-\tau_{\theta 0})$ and allows axial power transmission through the arterial wall.
(5) While radial wall motion reflects circumferential elasticity and circumferential initial tension, axial wall motion reflects axial elasticity and difference in initial tension $(\tau_{x0}-\tau_{\theta 0})$.

In the future, the four limitations in this study need to be addressed for improving our understanding of the relations of various pulsatile parameters with the four arterial wall mechanical properties, so that the calculated values of pulsatile parameters can be compared with the clinical data for quantitatively validating this theoretical study.

Funding Data

- Directorate for Engineering, National Science Foundation (NSF) (Grant No. 1936005; Funder ID: 10.13039/100000084).

References

[1] Au, J. S., Ditor, D. S., MacDonald, M. J., and Stöhr, E. J., 2016, "Carotid Artery Longitudinal Wall Motion is Associated With Local Blood Velocity and Left Ventricular Rotational, but Not Longitudinal, Mechanics," Physiol. Rep., **4**(14), p. e12872.
[2] Au, J. S., Bochnak, P. A., Valentino, S. E., Cheng, J. L., Stöhr, E. J., and MacDonald, M. J., 2018, "Cardiac and Haemodynamic Influence on Carotid Artery Longitudinal Wall Motion," Exp. Physiol., **103**(1), pp. 141–152.
[3] Taivainen, S. H., Yli-Ollila, H., Juonala, M., Kähönen, M., Raitakari, O. T., Laitinen, T. M., and Laitinen, T. P., 2018, "Influence of Cardiovascular Risk Factors on Longitudinal Motion of the Common Carotid Artery Wall," Atherosclerosis, **272**, pp. 54–59.
[4] Cinthio, M., Ahlgren, A. R., Bergkvist, J., Jansson, T., Persson, H. W., and Lindström, K., 2006, "Longitudinal Movements and Resulting Shear Strain of the Arterial Wall," Am. J. Physiol. Heart Circ. Physiol., **291**(1), pp. H394–H402.
[5] Taivainen, S. H., Yli-Ollila, H., Juonala, M., Kähönen, M., Raitakari, O. T., Laitinen, T. M., and Laitinen, T. P., 2017, "Interrelationships Between Indices of Longitudinal Movement of the Common Carotid Artery Wall and the Conventional Measures of Subclinical Arteriosclerosis," Clin. Physiol. Funct. Imaging, **37**(3), pp. 305–313.
[6] Yli-Ollila, H., Laitinen, T., Weckström, M., and Laitinen, T. M., 2016, "New Indices of Arterial Stiffness Measured From Longitudinal Motion of Common Carotid Artery in Relation to Reference Methods, a Pilot Study," Clin. Physiol. Funct. Imaging, **36**(5), pp. 376–388.
[7] Cardamone, L., Valentín, A., Eberth, J. F., and Humphrey, J. D., 2009, "Origin of Axial Prestretch and Residual Stress in Arteries," Biomech. Model. Mechanobiol., **8**(6), pp. 431–446.
[8] Humphrey, J. D., Eberth, J. F., Dye, W. W., and Gleason, R. L., 2009, "Fundamental Role of Axial Stress in Compensatory Adaptations by Arteries," J. Biomech., **42**(1), pp. 1–8.
[9] Nürnberger, J., Dammer, S., Opazo Saez, A., Philipp, T., and Schäfers, R. F., 2003, "Diastolic Blood Pressure is an Important Determinant of Augmentation Index and Pulse Wave Velocity in Young, Healthy Males," J. Hum. Hypertens., **17**(3), pp. 153–158.
[10] Willemet, M., and Alastruey, J., 2015, "Arterial Pressure and Flow Wave Analysis Using Time-Domain 1-D Hemodynamics," Ann. Biomed. Eng., **43**(1), pp. 190–206.
[11] Womersley, J. R., 1955, "XXIV. Oscillatory Motion of a Viscous Liquid in a Thin-Walled Elastic Tube—I: The Linear Approximation for Long Waves," London Edinburgh Dublin Philos. Mag. J. Sci., **46**(373), pp. 199–221.
[12] Atabek, H. B., 1968, "Wave Propagation Through a Viscous Fluid Contained in a Tethered, Initially Stresses, Orthotropic Elastic Tube," Biophys J., **8**(5), pp. 626–649.
[13] Mirsky, I., 1967, "Wave Propagation in a Viscous Fluid Contained in an Orthotropic Elastic Tube," Biophys. J.. **7**(2), pp. 165–86.

[14] Cox, R. H., 1969, "Comparison of Linearized Wave Propagation Models for Arterial Blood Flow Analysis," J Biomech., **2**(3), pp. 251–265.
[15] Klip, W., Van Loon, P., and Klip, D. A., 1967, "Formulas for Phase Velocity and Damping of Longitudinal Waves in Thick-Walled Viscoelastic Tubes," J. Appl. Phys., **38**(9), pp. 3745–3755.
[16] Holzapfel, G. A., and Ogden, R. W., 2010, "Constitutive Modelling of Arteries," Proc. R. Soc. A., **466**(2118), pp. 1551–1597.
[17] Humphrey, J. D., 2009, "Vascular Mechanics, Mechanobiology, and Remodeling," J. Mech. Med. Biol., **09**(02), pp. 243–257.
[18] Pinnington, R. J., and Briscoe, A. R., 1994, "Externally Applied Sensor for Axisymmetric Waves in a Fluid Filled Pipe," J. Sound Vib., **173**(4), pp. 503–516.
[19] Carew, T. E., Vaishnav, R. N., and Patel, D. J., 1968, "Compressibility of the Arterial Wall," Circ. Res., **23**(1), pp. 61–68.
[20] Anliker, M., Moritz, W. E., and Ogden, E., 1968, "Transmission Characteristics of Axial Waves in Blood Vessels," J. Biomech., **1**(4), pp. 235–246.
[21] Jagielska, K., Trzupek, D., Lepers, M., Pelc, A., and Zieliński, P., 2007, "Effect of Surrounding Tissue on Propagation of Axisymmetric Waves in Arteries," Phys. Rev. E Stat. Nonlinear Soft Matter Phys., **76**(6 Pt 2), p. 066304.
[22] Riley, W. A., Barnes, R. W., Evans, G. W., and Burke, G. L., 1992, "Ultrasonic Measurement of the Elastic Modulus of the Common Carotid Artery," Atheroscler. Risk Commun. (ARIC) Study. Stroke, **23**(7), pp. 952–956.
[23] Dobrin, P. B., 1978, "Mechanical Properties of Arteries," Physiol. Rev., **58**(2), pp. 397–460.
[24] Patel, D. J., Janicki, J. S., Vaishnav, R. N., and Young, J. T., 1973, "Dynamic Anisotropic Viscoelastic Properties of the Aorta in Living Dogs," Circ. Res., **32**(1), pp. 93–107.
[25] Al-Jumaily, A., and Lowe, A., 2013, "Accuracy of the Wave Equation in Predicting Arterial Pulse Propagation," Math. Comput. Modell., **57**(3–4), pp. 460–468.
[26] Yu, X., Wang, Y., and Zhang, Y., 2018, "Transmural Variation in Elastin Fiber Orientation Distribution in the Arterial Wall," J. Mech. Behav. Biomed. Mater., **77**, pp. 745–753.
[27] Li, D., and Robertson, A. M., 2009, "A Structural Multi-Mechanism Constitutive Equation for Cerebral Arterial Tissue," Int. J. Solids Struct., **46**(14–15), pp. 2920–2928.
[28] Qureshi, M. U., Colebank, M. J., Schreier, D. A., Tabima, D. M., Haider, M. A., Chesler, N. C., and Olufsen, M. S., 2018, "Characteristic Impedance: Frequency or Time Domain Approach?," Physiol. Meas., **39**(1), p. 014004.